Bulgarian Chemical Communications, Volume 58, Issue 2 (pp. 209-217) 2026 DOI: 10.34049/bcc.58.2.NCC05

Computational evaluation of bexarotene alkyl esters through DFT and molecular docking

N. A. Toshev[1*], I. R. Iliev[2], N. V. Agova[2], A. Abdollahi[3], S. F. Georgieva[2]

[1]*Medical University of Plovdiv, Faculty of Pharmacy, Department of Bioorganic Chemistry, 15A Vasil Aprilov Blvd., 4002 Plovdiv, Bulgaria*

[2]*Medical University Varna, Faculty of Pharmacy, Department of Pharmaceutical Chemistry, 84 Tsar Osvoboditel Blvd., 9000 Varna, Bulgaria*

[3]*Medical University of Plovdiv, Faculty of Medicine, 15A Vasil Aprilov Blvd., 4002 Plovdiv, Bulgaria*

Received: November 01, 2025; Revised: January 08, 2026

Bexarotene (Bex), a selective RXRα agonist approved by the U.S. Food and Drug Administration (FDA) for cancer treatment, is limited by poor aqueous solubility and suboptimal pharmacokinetic behavior. Structural modification *via* esterification with short-chain alcohols has been explored as a strategy to improve these properties. Methyl, ethyl, propyl, and butyl esters of Bex have been previously synthesized and characterized and they are commonly considered as potential prodrugs. However, existing data suggest that some of these derivatives may exhibit intrinsic biological activity or to hydrolysis, indicating a more complex pharmacodynamic profile. To further evaluate the suitability of esterification as a modification strategy, a comprehensive computational study was undertaken. Density Functional Theory (DFT) calculations at the B3LYP/6-311++G(d,p) level with implicit solvation (PCM) were employed to investigate the electronic properties of the esters, including descriptors such as HOMO–LUMO energy gap (ΔE), ionization potential (IP), electron affinity (EA), chemical hardness (η), chemical potential (μ), electronegativity (χ), electrophilicity index (ω), and maximum charge transfer index (ΔN max). Additionally, molecular docking simulations targeting the RXRα ligand-binding domain (PDB ID: 1FBY) were conducted to explore the binding potential and interaction profiles of the ester derivatives. The results provide insight into the molecular basis of receptor engagement and support a critical assessment of alkyl esterification as a rational strategy for enhancing the therapeutic profile of Bex. This theoretical framework offers a foundation for future design of bexarotene-based analogues and provides a conceptual basis for extending this approach beyond simple alkyl esters to include aryl derivatives.

Keywords: Bexarotene; alkyl esters; Density Functional Theory; molecular docking; RXRα; electronic descriptors

INTRODUCTION

Bexarotene (Bex) is a synthetic retinoid that selectively activates retinoid X receptors (RXRs) α, β, and γ, which act as transcription factors regulating genes involved in cellular differentiation, proliferation, apoptosis, and insulin sensitivity [1-3]. RXRs also form heterodimers with other nuclear receptors, contributing to their diverse biological functions [4-9]. The structural formula of Bex is shown in Fig. 1.

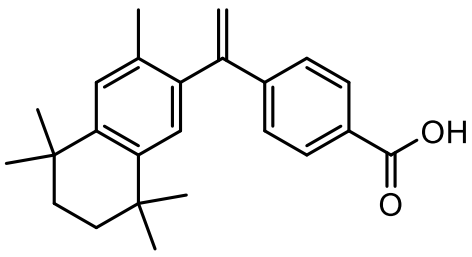

Figure 1. Structural formula of Bex.

Clinically, Bex is approved by the U.S. Food and Drug Administration (FDA) for the treatment of cutaneous T-cell lymphoma (CTCL) [4, 5, 9]. However, its therapeutic application is limited by poor aqueous solubility and suboptimal pharmacokinetic profile, both of which restrict its bioavailability and efficacy [9]. To overcome these limitations, various short-chain alkyl esters of Bex – methyl, ethyl, propyl, and butyl – have been synthesized and characterized.

The derivatives are frequently considered as potential prodrugs due to their ability to overcome the limitations associated with bexarotene. By modifying the chemical structure, these derivatives aim to improve pharmacokinetic properties, ultimately facilitating better absorption and target delivery in the treatment of the target receptors [10]. For the purpose of this study, they are denoted as E1 (methyl ester), E2 (ethyl ester), E3 (propyl ester), and E4 (butyl ester) throughout the text. The chemical structures of Bex alkyl esters are shown in Fig. 2.

* To whom all correspondence should be sent:
Email: *nikolay.toshev@mu-plovdiv.bg*

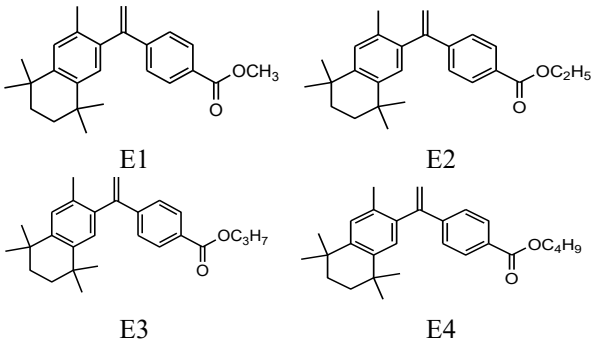

Figure 2. Chemical structures of Bex esters: E1 (methyl ester), E2 (ethyl ester), E3 (propyl ester), and E4 (butyl ester).

Although Bex has been extensively studied as a selective RXRα agonist, less is known about how esterification affects its electronic structure and receptor-binding potential. Understanding how alkyl substitution influences molecular reactivity and interaction with RXRα could support rational optimization of Bex derivatives.

Esterification is a well-established strategy for prodrugs that is often used to modify the lipophilicity, permeability, and pharmacokinetic behavior of bioactive compounds, including retinoids like bexarotene. While alkyl esters (such as methyl and butyl esters) are typically designed to undergo rapid enzymatic hydrolysis to release the parent drug, increasing evidence suggests that some ester derivatives can retain receptor affinity or exhibit measurable biological effects even before they are metabolized. These findings indicate that esterification does not always lead to pharmacologically inactive intermediates and may result in altered or additional pharmacodynamics properties. Therefore, computational approaches can be valuable tools for systematically assessing how esterification impacts molecular interactions and biological activity [11, 12].

In this study, we employed Density Functional Theory (DFT) and molecular docking analyses to investigate the relationship between electronic descriptors (HOMO–LUMO energy gap, electrophilicity index, dipole moment, etc.) and receptor affinity across the ester series. The aim was to determine whether computationally derived descriptors can predict biological performance and identify electronically favorable and pharmacologically relevant candidates for future development.

EXPERIMENTAL

Computational methodology -DFT study

The molecular orbitals Highest Occupied Molecular Orbital (HOMO) and Lowest Unoccupied Molecular Orbital (LUMO) were calculated using quantum chemistry methodology. All calculations were performed with the Gaussian 16 Rev. A.03 [13]. The combination between the B3LYP functional [14-16] and the 6-311++g (d, p) [17] basis set was chosen based on previous studies on carboxylic acids [18, 19]. The structures of the studied molecules were first optimized in the gas phase, and subsequently in water. All structures were optimized to a local minimum of potential energy, and no imaginary frequencies were found. PCM calculations in water (ε = 78) were applied to account for the effects of the solvation. The structures were visualized with the ChemCraft version 1.8.3 [20]. Global reactivity parameters that are derived from HOMO and LUMO energies provide additional interpretation of the results. Furthermore, data obtained from HOMO energies shed light on the molecule's capacity to act as an electron donor, while LUMO elucidates the potential as an electron acceptor. In this study, such descriptors as ionization potential ($IP = -E_{HOMO}$), electron affinity ($EA = -E_{LUMO}$), chemical potential ($\mu = 1/2 (E_{LUMO} + E_{HOMO})$), Mulliken electronegativity ($\chi = -\mu$), chemical hardness ($\eta = ½ (E_{LUMO} - E_{HOMO})$, softness ($\zeta = 1/\eta$), electrophilicity index ($\omega = \mu^2/2\eta$), and maximum charge transfer index (ΔN max) were calculated at the B3LYP/6-311+g(d,p) basis set for Bex and its alkyl esters in water.

Computational methodology - docking study

Ligand dataset preparation. Bex and its ester derivatives were selected as ligands for molecular docking with the human retinoid X receptor alpha (RXRα). The 3D structure of Bex was retrieved from the PubChem database [21]. The methyl and ethyl esters of Bex were obtained from the literature where they have been previously synthesized and characterized, while the propyl and butyl esters were generated in-house and structurally confirmed [10]. All ester derivatives were generated and converted into 3D structures using OpenBabel [22], followed by geometry optimization in Avogadro [23] with the MMFF94 force field. The optimized structures were saved in MOL2 format and further processed in AutoDock Tools [24], where polar hydrogens were added, Gasteiger charges were assigned, torsional degrees of freedom were defined, and ligands were saved in the PDBQT format for docking.

Reference ligand. 9-cis Retinoic acid, the natural ligand of RXRα, was included as a reference for validation of the docking protocol. Its 3D structure was obtained from the PubChem database (CID:

5282379), prepared using the same workflow as described for Bex and its esters.

Target protein preparation. The crystallographic structure of the human RXRα ligand-binding domain bound to 9-cis retinoic acid (PDB ID: 1FBY) [25] was retrieved from the RCSB Protein Data Bank [26]. Preprocessing was performed using UCSF ChimeraX [27], where chain B was removed due to its high structural similarity to chain A. All water molecules and non-standard residues were deleted. The protein was then imported into AutoDock Tools, where missing atoms were checked and repaired, polar hydrogens were added, Kollman charges were assigned, and atom types were set to AD4 specifications. The processed protein was saved in the PDBQT format for docking.

Flexible docking setup. To account for induced fit effects in the binding pocket, selected residues reported to be involved in ligand accommodation and stabilization within RXRα were defined as flexible: Phe313, Arg316, Ala271, Ala272, His435, Ile268, Ile345, Cys269, Ala327, Val342, and Cys432. The receptor side chains of these residues were allowed to rotate during docking, while the remaining protein was kept rigid.

Molecular docking protocol

Flexible docking simulations were carried out using AutoDock 4.2 with the Lamarckian Genetic Algorithm (LGA). The grid box was centered at coordinates x = 16.23, y = 27.27, z = 49.33 with dimensions of 60 × 60 × 60 points and a grid spacing of 0.375 Å, encompassing the entire ligand-binding pocket. Each docking run consisted of 100 independent LGA runs, with a population size of 300, a maximum of 25 000 000 energy evaluations, a mutation rate of 0.02, and a crossover rate of 0.8. Docked conformations were clustered using a root-mean-square deviation (RMSD) tolerance of 2.0 Å, and the lowest binding energy (ΔG) within the most populated cluster was selected as the representative binding pose.

Virtual screening analysis

Ligand–receptor interactions were examined in UCSF ChimeraX to evaluate binding orientation, hydrogen bonding, and hydrophobic contacts relative to the RXRα ligand-binding pocket. Two-dimensional interaction diagrams were generated using BIOVIA Discovery Studio Visualizer (Dassault Systèmes, San Diego, CA, USA) [28] to provide residue-level interpretation of binding interactions. Docking of 9-cis retinoic acid to RXRα served as internal validation of the docking protocol.

RESULTS AND DISCISSION

Density Functional Theory study

The optimized geometries of Bex and its alkyl esters, namely, the methyl (E1), ethyl (E2), propyl (E3), and butyl (E4) esters, are shown in Fig. 3.

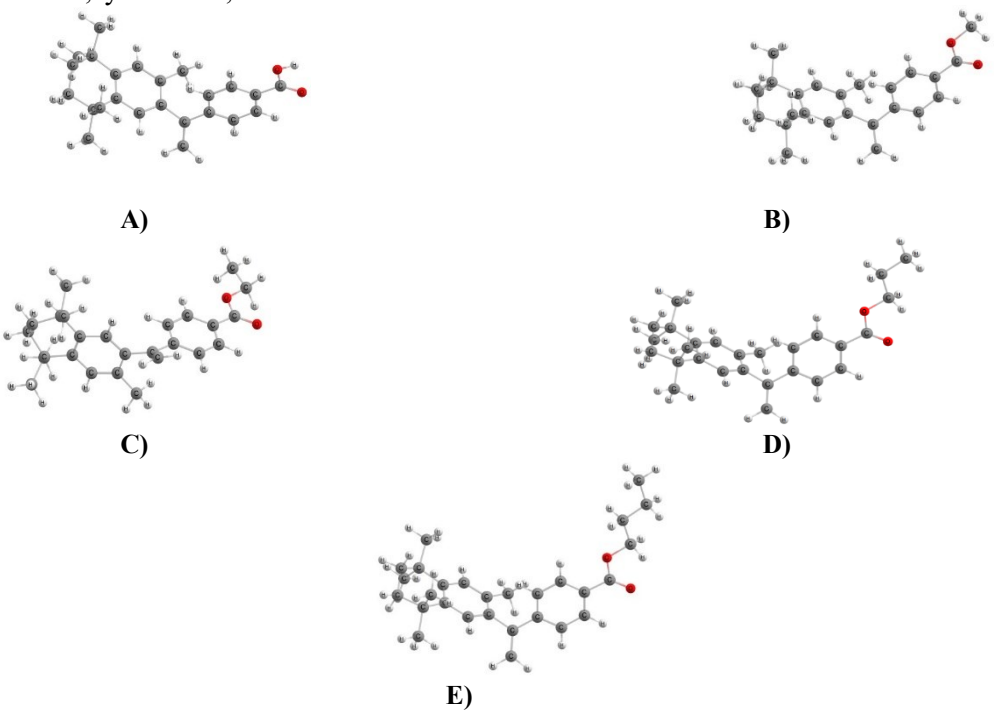

Figure 3. B3LYP/6-311++g (d, p) optimized structures in water of: A) Bex, B) Bex methyl ester (E1), C) Bex ethyl ester (E2), D) Bex propyl ester (E3), E) Bex butyl ester (E4).

Table 1. Energies (in eV) of the HOMO and LUMO, energy gap ΔE, ionization potential (IP), electron affinity (EA), electronegativity (χ), chemical potential (μ), chemical hardness (η), chemical potential (μ), electrophilicity index (ω), maximum charge transfer index (ΔN max), and dipole moment (D) calculated using the B3LYP/6-311+g (d, p) basis set for Bex and its alkyl esters in water.

	E_{HOMO}	E_{LUMO}	ΔE	IP	EA	χ	η	μ	ζ	ω	ΔN max	Dipole moment
Bexarotene	-6.36	-2.12	4.24	6.36	2.12	4.24	2.12	-4.24	0.47	4.24	2.00	3.99
Methyl ester (E1)	-6.35	-2.02	4.32	6.35	2.02	4.32	2.16	-4.19	0.46	4.05	1.94	3.77
Ethyl ester (E2)	-6.34	-2.01	4.34	6.34	2.01	4.34	2.17	-4.18	0.46	4.02	1.93	3.87
Propyl ester (E3)	-6.34	-2.01	4.34	6.34	2.01	4.34	2.17	-4.17	0.46	4.02	1.93	3.96
Butyl ester (E4)	-6.34	-2.00	4.34	6.34	2.00	4.34	2.17	-4.17	0.46	4.01	1.92	3.87

HOMO and LUMO analysis. The frontier molecular orbital (HOMO and LUMO) analysis of Bex and its alkyl esters provides useful information about the electronic structure and reactivity. Moreover, the energy gap between HOMO and LUMO sheds light on chemical reactivity and kinetic stability. The smaller the gap, the greater the decrease in kinetic stability, and higher chemical reactivity, as opposed to a higher gap, whereby the molecules have higher kinetic stability and lower chemical reactivity [29]. The HOMO and LUMO data for Bex and its alkyl esters are shown in Table 1.

Bex exhibits the highest occupied molecular orbital (HOMO) energy of -6.36 eV and the lowest unoccupied molecular orbital (LUMO) -2.12 eV, having an energy gap of 4.24 eV. In comparison, the ester derivatives show slight upward shifts in both HOMO and LUMO energies. The methyl ester has a HOMO -6.35 eV and a LUMO around 2.03 eV, thus yielding a gap of 4.32 eV. Similar energy gap was calculated for ethyl ester (4.34 eV), propyl ester (4.34 eV), and butyl ester (4.34 eV). As a result, the substitution of the -COOH group with -COOR increases the frontier energy orbital energies and slightly widens the HOMO-LUMO gap. Notably, the increase in the gap is most pronounced from the acid to the methyl ester (0.08 eV), while further increases in the length of the chain from methyl to butyl give around 0.02 eV. As a result, increasing the carbon chain through its inductive effect, does not significantly influence reactivity and stability. From a reactivity standpoint, Bex is expected to have higher reactivity compared to esters, esters having greater kinetic stability. In the context of drug molecules or candidates, a reduced band gap means that Bex has an enhanced ability to interact with biological targets compared to the ester derivatives. These findings align with prior studies conducted that, with an analogous series of compounds, suggest molecules with the smallest HOMO-LUMO gap tend to exhibit the highest activity or reactivity. In the context of drug candidates, reduced energy gaps correlate with increased biological and pharmacological activity; these molecules can more easily undergo charge-transfer reactions or bind to biological targets [30].

DFT descriptors analysis.

Bex showed the highest ionization potential (6.36 eV) and electronegativity (4.24 eV), demonstrating greater electronic stability compared to its esters. The alkyl esters exhibit slightly reduced ionization potential (6.34-6.35 eV) and electron affinity (2.02-2.00 eV). Moreover, the ionization potential (IP) and electron affinity (EA) values computed from HOMO and LUMO energies use Koopmans' theorem, which operates on fixed geometries and excludes structural relaxation after electron addition or removal. This approximation is widely used in DFT studies for rapid descriptor analysis; however, geometry relaxation may be missed. For this purpose, we ran an additional DFT calculation for the Bex to evaluate this effect. The adiabatic IP and EA were 6.05 eV and 2.56 eV, respectively, from the total energy differences between Bex, cationic, and anionic species. Compared to the Koopmans-based values (IP=6.36 eV, EA=2.12 eV), the differences were small: ΔIP= 0.31 eV and ΔEA= 0.44 eV. These results suggest that relaxation effects, while present, do not significantly alter the electronic effects. Thus, Koopmans-derived values represent a good approximation for this system, although full relaxation for all derivatives may improve descriptor precision. Bex has the lowest hardness of the series (η=2.12 eV); while esters are slightly higher in the series (η=2.17 eV), contrary to the hardness, the softness of the esters is higher than that of Bex. As a result, these differences, albeit subtle, underline the fact that the free acid is the "softest", whereas the

addition of alkyl substituents makes the molecules more rigid. Chemically, a softer molecule is more reactive, especially in polarizable interactions, while a harder molecule is more resistant to change [31]. Note that all these compounds have relatively high hardness (around 2 eV), which is a typical value for large conjugated organic molecules. From the perspective of chemical potential, which is negative to electronegativity, Bex is the most electrophilic, having negative chemical potential (-4.24 eV). The overall electronic stability is not significantly altered by esterification, supporting the idea that these modifications could be pharmacokinetically beneficial without severely affecting electronic potential.

The electrophilicity index (ω) describes a molecule's capacity to accept electron density and is linked with increased reactivity toward biological nucleophiles [31]. Weak electrophiles have an electrophilicity index $\omega < 0.8$ eV; moderate electrophiles have $0.8 < \omega < 1.5$; and strong electrophiles exhibit $\omega > 1.5$ eV [32]. Bex showed the highest value (4.24 eV), indicating a greater tendency to accept electrons compared to its ester derivatives. For the esters, the values were almost equal (4.01 – 4.05 eV), revealing that no remarkable change in electrophilicity index character is caused by esterification. This stability demonstrates that ester derivatives continue to exhibit enhanced reactivity towards biological nucleophilic targets. However, their stability suggests that they may be less reactive in biological pathways until they are metabolized.

The maximum charge transfer index (ΔN max) slightly decreased from Bex (2.00) to its butyl ester, indicating a small decrease in electron-donating capacity upon esterification. As a result of alkyl substitution, charge transfer potential is lowered, but all derivatives retain sufficient ability to engage in donor-acceptor interactions with biomolecular targets.

In terms of dipole moment, Bex demonstrated the largest dipole moment (3.99 D), showing a greater potential for solvation and polar reactions. The esters exhibited similar dipole moments (3.78-3.96 D), with propyl ester (3.96 D) closely matching with the parent molecule. This consistency confirms that polarity is well preserved during esterification, which is beneficial for maintaining solubility and interaction with polar residues in the RXRα binding site.

Overall, the DFT results indicate that esterification of Bex slightly increases the HOMO–LUMO gap without significantly altering its core electronic distribution. The large conjugated π-system common to all molecules dominates their electronic behavior, while ester substitution exerts only a minor local effect on frontier orbital energies and global reactivity parameters. This preservation of electronic features suggests that the alkyl esters may retain comparable electron density distribution and reactivity patterns to the parent compound, which is consistent with their potential to participate in similar molecular interactions or undergo metabolic conversion to Bex. This study used DFT calculations with the PCM implicit solvent model, which calculates solvent effects but does not account for individual hydrogen bonding interactions between the studied molecules and water. Note that this limitation may slightly affect the accuracy of descriptors, especially for more polar compounds. Modeling explicit water interactions enhances accuracy, but it is computationally demanding.

Molecular docking study

System preparation and method validation. The protein structure of the human RXRα ligand-binding domain (PDB ID: 1FBY) was prepared for docking by retaining only chain A, while chain B was removed due to its structural identity. Since both chains share an identical ligand-binding site, excluding chain B avoided redundancy and reduced computational complexity.

A set of key residues within the binding pocket was treated as flexible during docking to allow for more accurate modeling of ligand–receptor interactions. These included Phe313, Arg316, Ala271, Ala272, His435, Ile268, Ile345, Cys269, Ala327, Val342, and Cys432 which have been identified from the crystal structure and supported by literature data as critical for ligand recognition and stabilization [25].

To validate the docking protocol, a redocking experiment was performed using the reference ligand 9-cis retinoic acid, which is co-crystallized with 1FBY. The redocked pose yielded an RMSD of 3.14 Å compared to the crystallographic conformation, indicating acceptable reproducibility of the method.

Docking energy results. A summary of the docking outcomes for Bex, its ester derivatives, and the reference ligand 9-cis retinoic acid is presented in Table 2. The table reports the calculated binding free energy (ΔG), estimated inhibition constant (Ki), intermolecular energies, and torsional penalties for each ligand.

When comparing the docking results, all Bex esters exhibited stronger predicted binding affinities than the parent compound. Among them, the ethyl ester derivative showed the most favorable

Table 2. Docking results for Bex, its ester derivatives, and 9-cis retinoic acid with RXRα (PDB ID: 1FBY).

Parameter	Ref.	Bex	E1	E2	E3	E4
RMSD from reference structure, Å	3.14	55.112	54.656	54.595	54.703	59.276
Estimated free energy of binding (ΔG), kcal/mol	-10.64	-12.45	-13.25	-13.66	-13.40	-10.86
Estimated inhibition constant (Ki, 298.15 K)	15.96 nM	746.19 pM	194.74 pM	96.53 pM	149.85 pM	10.91 nM
Final intermolecular energy, kcal/mol	-12.43	-13.64	-14.44	-15.15	-15.19	-12.95
Ligand–fixed receptor, kcal/mol	-7.22	-5.06	-7.40	-7.99	-7.62	-7.88
- vdW+H-bond+desolvation, kcal/mol	-7.13	-4.94	-7.39	-7.96	-7.- 63	-7.88
- Electrostatic, kcal/mol	-0.09	-0.12	-0.01	-0.03	+0.02	0.00
Ligand–flexible residues, kcal/mol	-5.21	-8.58	-7.04	-7.16	-7.58	-5.07
- vdW+H-bond+desolvation, kcal/mol	-5.15	-7.89	-6.86	-7.00	-7.52	-5.07
- Electrostatic, kcal/mol	-0.05	-0.70	-0.18	-0.17	-0.06	0.00
Final total internal energy, kcal/mol	-8.98	-5.11	-10.53	-10.85	-9.70	-6.74
Ligand internal energy, kcal/mol	-1.18	-0.83	-0.84	-0.99	-0.94	-1.10
Ligand–fixed receptor, kcal/mol	-6.79	-3.59	-8.56	-8.43	-7.33	-6.28
Ligand–flexible residues, kcal/mol	-1.01	-0.70	-1.13	-1.42	-1.43	+0.64
Torsional free energy, kcal/mol	+1.79	+1.19	+1.19	+1.49	+1.79	+2.09
Unbound system energy, kcal/mol	-8.98	-5.11	-10.53	-10.85	-9.70	-6.74

interaction profile, with a binding free energy of -13.66 kcal/mol and the lowest inhibition constant (Ki = 96.53 pM), surpassing both Bex and the reference ligand 9-cis retinoic acid.

A clear trend was observed: increasing the length of the alkyl chain enhances hydrophobic interactions within the binding pocket, leading to more favorable intermolecular energies. However, this effect is counterbalanced by a progressive rise in the torsional free energy penalty, particularly for the longer-chain propyl and butyl esters. This indicates a trade-off between stability and conformational flexibility, with the ethyl ester providing the optimal balance.

The RMSD values for Bex and its ester derivatives were considerably higher than for 9-cis-retinoic acid, which can be attributed to the greater structural complexity and conformational flexibility of the polyaromatic framework of these molecules. Unlike the relatively rigid single-ring structure of the reference ligand, the extended and branched skeletons of Bex analogues allow multiple low-energy conformations, resulting in broader RMSD distributions during docking.

Interaction analysis (2D complexes)

The main intermolecular interactions between RXRα and all ligands were visualized using 2D interaction diagrams generated with Discovery Studio Visualizer, as shown in Figure 4. The docking poses revealed a consistent set of interactions between Bex and its ester derivatives with the RXRα binding pocket. Several key residues were identified as crucial for ligand stabilization:

- Hydrophobic and π-alkyl contacts: Phe313, Leu309, Ile268, Val342, Cys269, and Cys432 contributed significantly to the hydrophobic stabilization of the ligand.
- Hydrogen bonds: observed predominantly with Arg316 and Ala327, which were particularly evident in the methyl and ethyl ester derivatives, strengthening their binding affinity.
- π–Sulfur interactions: involving Cys269 and Cys432, further stabilized the aromatic core of the ligands and reinforced their orientation within the binding cavity.

A comparative analysis of the derivatives highlighted distinct patterns:

- Methyl and ethyl esters displayed enhanced hydrogen bonding capacity along with well-positioned hydrophobic interactions, resulting in superior binding profiles.
- Propyl and butyl esters demonstrated stronger hydrophobic contacts due to their extended alkyl chains, but this was counterpoised by a higher torsional energy penalty, reflecting reduced conformational efficiency.

When compared with the reference ligand 9-cis retinoic acid, both Bex and its esters demonstrated

more extensive hydrophobic contacts. Although 9-cis retinoic acid engaged in hydrogen bonding, its overall weaker hydrophobic interactions accounted for the less favorable binding free energy and higher inhibition constant (Ki = 15.96 nM).

SAR analysis

The docking results provide valuable insights into the structure–activity relationship (SAR) of Bex and its ester derivatives. The carboxyl group of the parent compound enables strong ionic and hydrogen-bonding interactions; however, upon esterification, this capacity is reduced. Instead, the ester derivatives benefit from enhanced hydrophobic contacts within the binding cavity, leading to lower binding free energies (ΔG).

Increasing the length of the alkyl chain further strengthens hydrophobic interactions, which is reflected in the improved binding affinities of the methyl, ethyl, and propyl esters compared to the parent ligand. Nevertheless, this effect appears to have a limit: the butyl ester did not exceed the ethyl derivative, suggesting that excessive chain elongation introduces steric strain and higher torsional penalties, diminishing the overall benefit. Taken together, the results confirm that small to medium-sized ester substitutions are optimal for improving the binding affinity of Bex analogues toward RXRα, balancing hydrophobic stabilization with conformational flexibility.

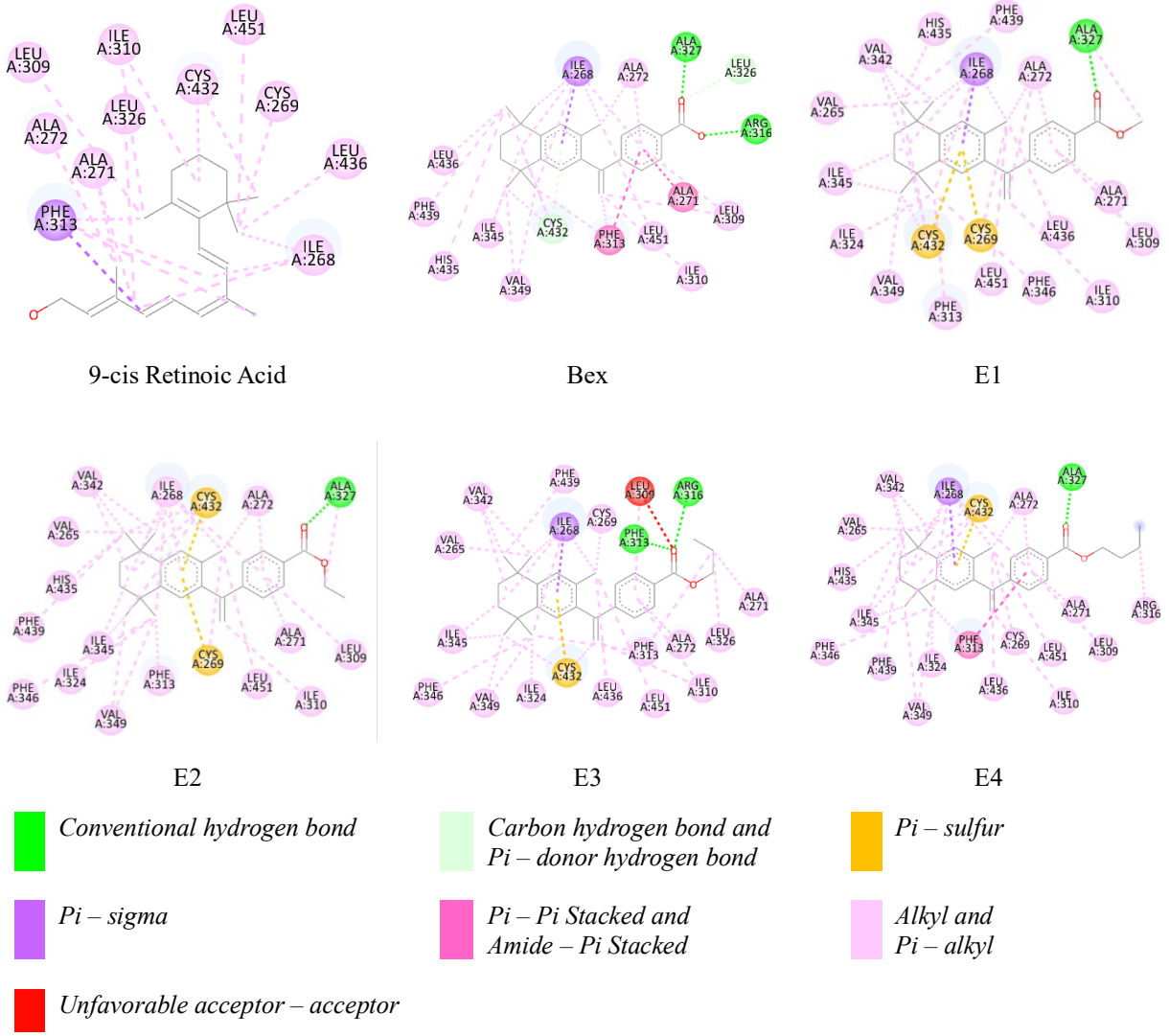

Figure 4. Two-dimensional interaction diagrams of the RXRα–ligand complexes showing key amino acid contacts for 9-cis retinoic acid (Ref), Bexarotene, and its methyl (E1), ethyl (E2), propyl (E3), and butyl (E4) esters. Hydrophobic interactions, hydrogen bonds, and π–sulfur contacts are indicated by standard color codes and symbols as generated by Discovery Studio Visualizer.

Biological interpretation

The markedly lower inhibition constants (Ki) observed for the ester derivatives—within the picomolar range – compared to the nanomolar affinity of 9-cis retinoic acid highlight their potential as highly potent RXRα ligands.

These findings suggest that Bex esters may serve as alternative RXRα agonists with improved binding capabilities relative to both the parent compound and the endogenous reference ligand. Their enhanced hydrophobic stabilization within the receptor's binding pocket supports the hypothesis of stronger and more sustained receptor activation.

Furthermore, the ester derivatives may function as prodrugs, undergoing metabolic hydrolysis to regenerate the active carboxylic acid form of Bex *in vivo* [10]. This dual mechanism – direct receptor engagement by the ester and potential conversion to the acid – could provide therapeutic advantages, such as modulated pharmacokinetics and improved bioavailability.

CONCLUSION

Based on density functional theory and docking calculations, a systematic theoretical study of Bex and its alkyl esters has been carried out. Esterification of Bex leads to increased HOMO-LUMO energy gaps (4.32-4.34 eV), indicating decreased electronic reactivity of the esters compared to Bex. Nevertheless, this shows that esterification does not produce a significant effect on the electronic properties or the overall electron density distribution of esters. The dipole moments were consistent throughout the series, with Bex having a slightly higher polarity (3.99 D) compared to its methyl (3.78 D) and ethyl (3.87 D) esters. Among the derivatives, the ethyl ester displayed a dipole moment, chemical softness, and ionization energy, closely aligning to Bex. Despite lower reactivity, docking studies revealed enhanced RXRα binding for all esters, especially the ethyl ester, which exhibited the strongest binding affinity (-13.66 kcal/mol, Ki=96.53 pM). These results indicate that improved binding is related not only to polarity or electrophilicity index, but also to favorable hydrophobic interactions and optimal ligand flexibility. The moderate electrophilicity index (4.02 eV), along with preserved polarity and improved docking performance, highlights ethyl ester as a promising lead compound. Note that the large conjugated system that is common for all studied molecules is predominant in the electronic structure compared to the possible carboxylic group modification, thus affecting the behavior of these molecules in a biological context. The combined DFT study and docking analyses suggest that Bex ethyl ester may offer improved receptor engagement, supporting its potential as an optimized RXRα ligand that retains essential electronic features of the parent molecule while exhibiting physicochemical properties consistent with possible metabolic interconversion to Bex. However, these computational predictions require experimental validation, and further *in vitro* RXR binding assays will be essential to confirm the observed trends and assess their biological significance.

Acknowledgement: *The research that led to these results was carried out using the infrastructure purchased under the national Roadmap for RI financially coordinated by the MES of the Republic of Bulgaria (grant № D01-98/26.06.2025). The computation was performed by shared resource with GAUSSIAN 16 by project KP-06-N59/7(project leader Vassil Delchev).*

REFERENCES

1. K. Tomita, K. Nakashima, E. Yamaguchi, A. Itoh, K. Tsutsumiuchi, M. Inoue, *Mol. Pharmacol.*, **107** (8), 100057 (2025).
2. F. Lalloyer, C. Fiévet, S. Lestavel, G. Torpier, J. van der Veen, V. Touche, S. Bultel, A. Tailleux, *Arterioscler. Thromb. Vasc. Biol.*, **26** (12), 2731 (2006).
3. M. Certo, Y. Endo, K. Ohta, S. Sakurada, G. Bagetta, D. Amantea, *Pharmacol. Res.*, **102**, 298 (2015).
4. L. T. Farol, K. B. Hymes, *Expert Rev. Anticancer Ther.*, **4** (2), 180 (2004).
5. L. Qu, X. Tang, *Cancer Chemother. Pharmacol.*, **65** (2), 201 (2010).
6. H. Cao, R. Bissinger, A. T. Umbach, M. Gawaz, F. Lang, *Cell. Physiol. Biochem.*, **42** (2), 838 (2017).
7. T. W. Hermann, W.-C. Yen, P. Tooker, B. Fan, K. Roegner, A. Negro-Vilar, W. W. Lamph, R. P. Bissonnette, *Lung Cancer*, **50** (1), 9 (2005).
8. C. Hacioglu, F. Kar, S. Kacar, V. Sahinturk, G. Kanbak*Med. Oncol.*, **38**, 31 (2021).
9. A. Mahajan, L. Singh, G. Singh, R. K. Dhawan, M. Kaur, P. K. Malhi, K. Thakur, L. Kaur, An evidence-based review on bexarotene, *Tumor Discov.*, **2** (2), 0436 (2023).
10. I. Iliev, S. Georgieva, *Bulg. Chem. Commun.*, **56** (Spec. Issue D1), 77 (2024).
11. J. B. Lee, A. Zgair, J. Malec, T. H. Kim, M. G. Kim, J. Ali, C. Qin, W. Feng, M. Chiang, X. Gao, G. Voronin, A. E. Garces, C. L. Lau, T.-H. Chan, A. Hume, T. M. McIntosh, F. Soukarieh, M. Al-Hayali, E. Cipolla, H. M. Collins, D. M. Heery, B. S. Shin, S. D. Yoo, L. Kagan, M. J. Stocks, T. D. Bradshaw, P. M. Fischer, P. Gershkovich, *Journal of Controlled Release*, **286**, 10 (2018).
12. K. Beaumont, R. Webster, I. Gardner, K. Dack*Current Drug Metabolism*, **4** (6), 461 (2003)

13. M. J. Frisch, G. W. Trucks, H. B. Schlegel, G. E. Scuseria, M. A. Robb, J. R. Cheeseman, G. Scalmani, V. Barone, G. A. Petersson, H. Nakatsuji, X. Li, M. Caricato, A. V. Marenich, J. Bloino, B. G. Janesko, R. Gomperts, B. Mennucci, H. P. Hratchian, J. V. Ortiz, A. F. Izmaylov, J. L. Sonnenberg, D. Williams, F. Ding, F. Lipparini, F. Egidi, J. Goings, B. Peng, A. Petrone, T. Henderson, D. Ranasinghe, V. G. Zakrzewski, J. Gao, N. Rega, G. Zheng, W. Liang, M. Hada, M. Ehara, K. Toyota, R. Fukuda, J. Hasegawa, M. Ishida, T. Nakajima, Y. Honda, O. Kitao, H. Nakai, T. Vreven, K. Throssell, J. A. Montgomery Jr., J. E. Peralta, F. Ogliaro, M. J. Bearpark, J. J. Heyd, E. N. Brothers, K. N. Kudin, V. N. Staroverov, T. A. Keith, R. Kobayashi, J. Normand, K. Raghavachari, A. P. Rendell, J. C. Burant, S. S. Iyengar, J. Tomasi, M. Cossi, J. M. Millam, M. Klene, C. Adamo, R. Cammi, J. W. Ochterski, R. L. Martin, K. Morokuma, O. Farkas, J. B. Foresman, D. J. Fox, Gaussian 16 Rev. C.01, Gaussian, Inc., Wallingford CT, 2016.
14. A. D. Becke, *J. Chem. Phys.*, **98**, 5648 (1993).
15. A. D. Becke, *J. Chem. Phys.*, **104**, 1040 (1996).
16. C. Lee, W. Yang, R. G. Parr, *Phys. Rev. B*, **37**, 785 (1988).
17. R. Krishnan, J. S. Binkley, R. Seeger, J. A. Pople, Self-consistent molecular orbital methods. XX. A basis set for correlated wave functions, *J. Chem. Phys.*, **72**, 650 (1980).
18. M. Karabacak, Z. Cinar, M. Kurt, S. Sudha, N. Sundaraganesan, *Spectrochim. Acta A Mol. Biomol. Spectrosc.*, **85** (1), 179 (2012).
19. T. Kaweetirawatt, Y. Kokita, S. Iwai, M. Sumimoto, K. Hori, *Chem. Phys. Lett.*, **547**, 97 (2012).
20. Chemcraft—graphical software for visualization of quantum chemistry computations, Version 1.8 (Build 682), Chemcraft, 2010.
21. National Center for Biotechnology Information (NCBI), U.S. National Library of Medicine, available at: https://www.ncbi.nlm.nih.gov/
22. N. M. O'Boyle, M. Banck, C. A. James, C. Morley, T. Vandermeersch, G. R. Hutchison, *J. Cheminform.*, **3**, 33 (2011).
23. M. D. Hanwell, D. E. Curtis, D. C. Lonie, T. Vandermeersch, E. Zurek, G. R. Hutchison, *J. Cheminform.*, **4**, 17 (2012).
24. G. M. Morris, R. Huey, W. Lindstrom, M. F. Sanner, R. K. Belew, D. S. Goodsell, A. J. Olson, *J. Comput. Chem.*, **30**, 2785 (2009).
25. P. F. Egea, A. Mitschler, N. Rochel, M. Ruff, P. Chambon, D. Moras, *EMBO J.*, **19**, 2592 (2000).
26. RCSB Protein Data Bank (RCSB PDB), U.S. National Library of Medicine, available at: https://www.rcsb.org/
27. R. J. Read, E. F. Pettersen, A. J. McCoy, T. I. Croll, T. C. Terwilliger, B. K. Poon, E. C. Meng, D. Liebschner, P. D. Adams, *Acta Crystallogr. D: Struct. Biol.*, **80**, 588 (2024).
28. U. Baroroh, Z. S. Muscifa, W. Destiarani, F. G. Rohmatullah, M. Yusuf, *J. Comput. Biol.*, **2**, 22 (2023).
29. K. Fukui, S*cience*, **218**, 747 (1982).
30. S. K. Misra, G. Ghoshal, M. R. Gartia, Z. Wu, A. K. De, M. Ye, C. R. Bromfield, E. M. Williams, K. Singh, K. V. Tangella, *ACS Nano*, **9**, 10695 (2015).
31. R. G. Parr, R. G. Pearson, *J. Am. Chem. Soc.*, **105**, 7512 (1983).
32. L. R. Domingo, M. J. Aurell, P. Pérez, R. Contreras, *Tetrahedron*, **58**, 4417 (2002).